Continuum Mech. Thermodyn. (2020) 32:127–146
https://doi.org/10.1007/s00161-019-00791-1

ORIGINAL ARTICLE

Bruno Musil · Martin Böhning · Michael Johlitz · Alexander Lion

On the inhomogenous chemo-mechanical ageing behaviour of nitrile rubber: experimental investigations, modelling and parameter identification

Received: 23 January 2019 / Accepted: 21 May 2019 / Published online: 28 May 2019

Abstract Elastomers are used in almost all areas of industrial applications, such as tires, engine mounts, bridge bearings, seals or coatings. During their use in operation, they are exposed to different environmental influences. These include, in particular, climatic factors such as air oxygen, high temperatures, light (UV radiation) and the influence of media (e.g. oils, fuels). A very important result of these factors is the chemical ageing of elastomers. In this case, the elastomer degenerates and changes its chemical structure in the aged regions, which leads to an irreversible change in the material properties in connection with the reduction in its usability. In this paper, chemical ageing of nitrile butadiene rubber (NBR) is investigated. Especially in case of thermo-oxidative ageing at elevated operating temperatures, the ageing processes run inhomogeneously. These effects are known as diffusion-limited oxidation (DLO) and are associated with the diffusion–reaction behaviour of atmospheric oxygen with the elastomer network. For these reasons, NBR samples are artificially aged in air and subjected to different experimental methods, which are presented and discussed. Additional results from inhomogeneous mechanical tests and permeation tests indicate the causes of the DLO-effect, show the influence of chemical ageing and are subsequently used for parameter identification in relation to the diffusion–reaction equation. A continuum-mechanical modelling approach is also presented here, which describes the finite hyperelasticity, diffusion–reaction processes as well as chemical degradation and reformation of the elastomer network. This multifield problem leads to a system of partial and ordinary differential equations and constitutive equations and is solved within the finite element method.

Keywords Chemical ageing · NBR · Hyperelasticity · DLO

1 Introduction and stay of the art

In recent years, elastomers and elastomer components have been more and more used in industrial applications, which leads to increased demands on their applicability and durability. In addition to the chemical side of preparing and vulcanizing the compound, the optimization and consideration of the relevant external influences plays an important role in designing of elastomer components. These influences can occur during operation and thus significantly contribute to the impairment of the mechanical and other important material properties. Such factors include elevated operating temperatures, influence of oxygen (oxidation) and other media (e.g. oils, fuels), influence of solar radiation (UV radiation), mechanical loading, etc. (cf. [8]).

Communicated by Andreas Öchsner.

B. Musil (✉) · M. Johlitz · A. Lion
Institute of Mechanics, Universität der Bundeswehr München, Werner-Heisenberg-Weg 39, 85579 Neubiberg, Germany
E-mail: bruno.musil@unibw.de

M. Böhning
Bundesanstalt für Materialforschung und -prüfung (BAM), Unter den Eichen 87, 12205 Berlin, Germany

An important result of these factors is the chemical ageing of elastomers. In this case, the elastomer degenerates and changes its chemical structure in the aged regions, which leads to an irreversible change in the material properties in connection with the reduction in its usability. As it is widely known, chemical ageing of elastomers results in irreversible changes in the internal structure of the network. Influences of external media lead to scission of the primary network of the elastomer and thus to its degradation. In parallel, there is the creation of new network junctions, which is often called network reformation or cross-linking (cf. [3,26,30]).

However, chemical ageing processes, especially in case of thermo-oxidative ageing, run in general inhomogeneously. In order to trigger the chemical ageing, the elastomer needs a reaction partner such as oxygen. The rate of the degeneration process is limited by the surrounding media's diffusivity and the reaction speed of the elastomer and the medium. For very thin samples or parts (e.g. coatings, membranes), one can consider a homogenous saturation with oxygen. The only parameter limiting the duration of the ageing process is then the reactivity of the elastomer and the ageing reactant, which depends on the temperature (cf. [7]). In many industrial applications, components of larger dimensions are used so that diffusion-limited oxidation (DLO) needs to be considered. DLO can occur whenever the rate of oxygen consumption within the material is greater than the rate at which it can be resupplied by diffusion from the surrounding medium. This can lead to a heterogeneously oxidized material. The so-called equilibrium oxidation occurs only at the surfaces, and a reduced or none oxidation occurs in interior regions (cf. [2,11]). For these reasons, the thermo-oxidative ageing is regarded as inhomogeneous.

The thermo-oxidative ageing of elastomers is based on chemical processes that proceed according to a modelling concept known as basic autooxidation scheme (BAS) (cf. [4]). This scheme is based on the reactions of free radicals of the elastomer chains with oxygen. In the works of [10,32], BAS was taken as a basis which has been adapted to stabilized elastomers used in industrial applications. Under certain assumptions, they were able to determine a linear relationship between the oxygen concentration and its consumption rate from the modified BAS. So, only one material parameter (reaction parameter) has to be determined here.

In several studies, the DLO-effect resp. inhomogeneous ageing of elastomers has been experimentally investigated and modelled from the mechanical point of view. In [21,28] or [23], the diffusion–reaction equation for oxygen as a trace element is solved. The reactions based on the BAS were considered, in order to calculate an oxygen concentration profile in an elastomer component. The diffusion–reaction model was coupled with the change in material behaviour via phenomenological approaches, such that the authors were able to depict the DLO-effect. In [16], a diffusion–reaction equation is also solved. This approach based on the formulation of the multiphase problem, such that a consistent thermodynamic evaluation of the equations according to the entropy principle by Liu–Müller was carried out. The theory was presented in the context of linear viscoelasticity. In a later work by Dippel et al. [6], the material model proposed by Johlitz and Lion [16] was adapted to finite strains and illustrated using the example of ageing of polymer bonds.

To identify the reaction parameters of diffusion–reaction equations, several methods have been developed. The direct method of measurement represents a measurement of the oxygen consumption of the elastomer during the thermo-oxidative ageing by a respirometric method (cf. [12,22,29]). Indirect measurements are also possible. In [21,32], modulus profiling as an indicator of the DLO-effect was used with good results. However, the disadvantage lies in the demanding sample preparation as well as in the fact that the relations between the measured local micro-hardness and the reacted oxygen are empirically formulated.

This paper deals with the continuum-mechanical modelling and experimental investigation of the inhomogeneous thermo-oxidative ageing of nitrile rubber. A chemo-mechanical material model, within the framework of finite hyperelasticity, is introduced and its parameters are identified (mechanical parameters, ageing parameters and parameters of the diffusion–reaction equation). Modelling the ageing of elastomers is done with two internal variables $q_{\mathrm{d}}\,(\mathbf{X}, t, \theta, \dots)$, $q_{\mathrm{r}}\,(\mathbf{X}, t, \theta, \dots)$ which describe the resulting network modification processes occurring during ageing. This concept has already been used in a similar way in [14,15,20]. Thereby, the variable q_{d}, which represents the chain scission, equals to zero for the initial state and is one for the fully aged state. The second variable q_{r}, representing the network reformation, operates the other way around and is equal to zero in case of unaged elastomer and develops to one for the fully aged state. In [16], the evolution of the two inner variables is strongly influenced by the oxygen concentration, which allows to consider the effect of heterogeneous oxidation on the material behaviour.

Since the diffusion of oxygen into the elastomer is an essential part of the thermo-oxidative ageing, the dependence of the diffusion coefficient of oxygen in the elastomer on ageing is also experimentally investigated and considered in the modelling approach within this paper. For this purpose, so-called permeation tests (cf. [5,25]) on unaged and aged NBR specimens are carried out.

The focus here is also based on the identification of the material parameters of the diffusion–reaction equation. In this study, an indirect identification method is used to determine the local oxygen consumption in an elastomer component. In contrast to the above strategy using modulus profiling, a part (specimen) is artificially aged in air and then cut into a number of thin samples. With such samples, one can perform a suitable mechanical experiment, resulting in an inhomogeneous stress profile across the elastomer component, which is subsequently available for parameter identification by means of inverse FEM and combination with a nonlinear optimization method. Accordingly, no empirical approaches are necessary and the reaction parameters can be identified directly using the implemented chemo-mechanical material model, so that the error between measurement and simulation is minimized.

2 Theory and modelling

In terms of modelling, the following assumptions were made: Both the unaged and aged elastomer exhibit a mechanically incompressible behaviour. No temperature gradients are considered, so that an isothermal as well as an adiabatic state is assumed. Furthermore, it is postulated that the evolution of ageing is strain-independent, which has been experimentally shown for some rubbers (cf. [17,30]). Ageing is described in a phenomenological way by the internal variables q_d, q_r, whose evolution may dependent on the local oxygen concentration.

Regarding the general motion of a deformable body, the concept of the multiplicative split of the deformation gradient tensor $\mathbf{F}$ is considered (cf. [9,19]), whereby a split $\mathbf{F} = \bar{\mathbf{F}} \cdot \hat{\mathbf{F}}$ into a volumetric part $\bar{\mathbf{F}}$ and isochoric part $\hat{\mathbf{F}}$ is considered, which motivates a volumetric-isochoric intermediate configuration. The right Cauchy-Green deformation tensor $\mathbf{C} = \mathbf{F}^T \cdot \mathbf{F}$ and the Green-Lagrangian strain tensor $\mathbf{E} = \frac{1}{2}(\mathbf{C} - \mathbf{I})$ operate on the reference configuration.

For oxygen as a trace element, the local mass balance, in other words the diffusion–reaction equation, reads as follows

$$\rho_0 \, \dot{c} + \mathrm{Div}\, \mathbf{j} - \hat{c} = 0, \tag{1}$$

which describes the change of oxygen in space and time. Here, c represents the dimensionless oxygen concentration (see Eq. (24)), $\mathbf{j}$ is the oxygen flux and $\hat{c}$ is the reaction term. The quasi-static balance of momentum for the elastomer is

$$\mathrm{Div}\, \mathbf{P} = 0, \tag{2}$$

where $\mathbf{P}$ is the first Piola-Kirchhoff stress tensor. Two further balance equations are considered. The balance of internal energy e is formulated for isothermal processes without radiation

$$\rho_0 \, \dot{e} = \mathbf{S} : \dot{\mathbf{E}}. \tag{3}$$

In this balance, $\mathbf{S}$ represents the second Piola-Kirchhoff stress tensor. Finally, the entropy inequality is formulated

$$\rho_0 \, \dot{s} + \mathrm{Div}\, \boldsymbol{\Phi}^s - \rho_0 \, \eta^s = \rho_0 \, \hat{\eta} \geq 0, \tag{4}$$

which describes the non-negative entropy production during a process. This inequality includes the temporal change of the specific entropy s, the entropy flux $\boldsymbol{\Phi}^s$, the entropy supply η^s and the entropy production $\hat{\eta}$. In [16], the approach

$$\begin{aligned} \eta^s &= \frac{r}{\theta} = 0 \\ \boldsymbol{\Phi}^s &= -\frac{1}{\theta} \frac{\partial \psi}{\partial c} \mathbf{j} \end{aligned} \tag{5}$$

for the variables of the entropy inequality was motivated. After inserting Eq. (5) into the inequality (4) and using the Legendre transformation, $\psi = e - \theta \, s$, and the energy balance (3), yields the following equation

$$-\rho_0 \, \dot{\psi} + \mathbf{S} : \dot{\mathbf{E}} - \mathbf{j} \cdot \mathrm{Grad} \frac{\partial \psi}{\partial c} - \frac{\partial \psi}{\partial c} \mathrm{Div}\, \mathbf{j} \geq 0. \tag{6}$$

This equation defines the final formulation of the Clausius–Duhem inequality to be fulfilled by the material model. It requires the non-negativity of the total entropy production and considers in particular the flux of entropy caused by the diffusing oxygen.

The independent variables of this multifield problem are the concentration c and the deformation $\mathbf{C}$; on the other hand, the variables for which constitutive equations have to be formulated are

$$\Pi := \left\{\mathbf{j},\ \hat{c},\ \mathbf{S}\right\}. \tag{7}$$

According to the equipresence rule, all variables Π depend on the same set of independent variables, which are chosen as

$$\Pi = \hat{\Pi}\left\{c,\ \mathbf{C},\ q_\mathrm{d},\ q_\mathrm{r}\right\}. \tag{8}$$

According to [16], an additive split of the specific Helmholtz free energy ψ in a mechanical and a chemical part is motivated

$$\begin{aligned} \psi &= \psi_\mathrm{mech}\left(\mathbf{C},\ q_\mathrm{d},\ q_\mathrm{r}\right) + \psi_\mathrm{c}(c) \\ \psi_\mathrm{mech} &= \psi_\mathrm{vol} + \psi_\mathrm{d} + \psi_\mathrm{r}. \end{aligned} \tag{9}$$

The mechanical part of the free energy density is further additively split into the volumetric part ψ_vol, the degradative part ψ_d and on the part ψ_r that contains the network reformation process. The volumetric part is chosen according to [27]. For ψ_d, a Neo-Hookean approach is used. The reforming network builds up stress-free under constant strain. Therefore, a hypoelastic formulation is used, with the corresponding part of the free energy function in integral form as a history functional (cf. [13,20]). Hence, contributions to the specific free energy are:

$$\begin{aligned} \rho_0\,\psi_\mathrm{vol} &= \frac{1}{2}\,K\left[(J-1)^2 + (\ln J)^2\right] \\ \rho_0\,\psi_\mathrm{d} &= \frac{1}{2}\,\mu(q_\mathrm{d})\left(I_{\hat{\mathbf{C}}} - 3\right) \\ \rho_0\,\psi_\mathrm{r} &= \frac{1}{2}\int_0^t \left([\overset{4}{\mathbf{D}}(s)\ q_\mathrm{r}(s)]' : [\mathbf{E}(t) - \mathbf{E}(s)]\right) : [\mathbf{E}(t) - \mathbf{E}(s)]\,\mathrm{d}s. \end{aligned} \tag{10}$$

In Eq. (10)$_2$ $I_{\hat{\mathbf{C}}}$ represents the first invariant of the isochoric right Cauchy–Green deformation tensor $\hat{\mathbf{C}} = J^{-2/3}\,\mathbf{C}$. To simulate the mechanical incompressibility of the material, the choice of the bulk modulus K has to be approximately three orders of magnitude higher than the shear modulus. The time derivative of ψ results to

$$\begin{aligned} \rho_0\,\dot{\psi}_\mathrm{vol} &= \frac{J}{2}\,K\left[(J-1) + \left(\frac{1}{J}\,\ln J\right)\right]\mathbf{C}^{-1} : \dot{\mathbf{C}} \\ \rho_0\,\dot{\psi}_\mathrm{d} &= \frac{1}{2}\,\mu(q_\mathrm{d})\left(\mathbf{I} - \frac{1}{3}\,I_\mathbf{C}\,\mathbf{C}^{-1}\right) : \dot{\mathbf{C}} + \frac{\partial \rho_0\,\psi_\mathrm{d}}{\partial q_\mathrm{d}}\,\dot{q}_\mathrm{d} \\ \rho_0\,\dot{\psi}_\mathrm{r} &= \int_0^t [\overset{4}{\mathbf{D}}(s)\ q_\mathrm{r}(s)]' : [\mathbf{E}(t) - \mathbf{E}(s)]\,\mathrm{d}s\ : \dot{\mathbf{E}}. \end{aligned} \tag{11}$$

Thus, using the relation $\dot{\mathbf{E}} = 1/2\,\dot{\mathbf{C}}$, the second law of thermodynamics in form of Eq. (6) can be evaluated by standard methods and leads to the following constitutive equations for the stress tensor

$$\begin{aligned} \mathbf{S} &= \mathbf{S}_\mathrm{vol} + \mathbf{S}_\mathrm{d} + \mathbf{S}_\mathrm{r} \\ \mathbf{S}_\mathrm{vol} &= J\,K\left[(J-1) + \left(\frac{1}{J}\,\ln J\right)\right]\mathbf{C}^{-1} \\ \mathbf{S}_\mathrm{d} &= \mu(q_\mathrm{d})\,J^{-\frac{2}{3}}\left(\mathbf{I} - \frac{1}{3}\,I_\mathbf{C}\,\mathbf{C}^{-1}\right) \\ \mathbf{S}_\mathrm{r} &= \int_0^t [\overset{4}{\mathbf{D}}(s)\ q_\mathrm{r}(s)]' : [\mathbf{E}(t) - \mathbf{E}(s)]\,\mathrm{d}s. \end{aligned} \tag{12}$$

One can see that the stress tensor $\mathbf{S}$ has a modular structure. It is additively split into the volumetric part $\mathbf{S}_\mathrm{vol}$, the degradative part $\mathbf{S}_\mathrm{d}$ and the reformative part $\mathbf{S}_\mathrm{r}$. Regarding the reformative part, the integral form of the stress tensor $\mathbf{S}_\mathrm{r}$ is reformulated by using the time differentiation

$$\dot{\mathbf{S}}_\mathrm{r} = \frac{1}{2}\,q_\mathrm{r}(t)\ \overset{4}{\mathbf{D}} : \dot{\mathbf{C}} \tag{13}$$

to the hypoelastic formulation. This rate formulation of the constitutive equation guarantees a stress-free network reformation. The fourth-order stiffness tensor is defined as

$$\overset{4}{\mathbf{D}} = 4\,\frac{\partial^2 w}{\partial \mathbf{C}^2} \tag{14}$$

where

$$w = \frac{1}{2}\,\mu_{\mathrm{r}}\left(I_{\hat{\mathbf{C}}} - 3\right) \tag{15}$$

represents the strain energy density of the network reformation process, in which μ_{r} is the shear modulus of the reformed elastomer network. In Eq. (14), the second partial derivative of w reads as follows

$$\begin{aligned}\frac{\partial^2 w}{\partial \mathbf{C}^2} = \frac{1}{2}\,\mu_{\mathrm{r}}\,J^{-\frac{2}{3}}\,\frac{1}{3}\Bigg[I_{\mathbf{C}}\left(\frac{1}{3}\,\mathbf{C}^{-1}\otimes\mathbf{C}^{-1} + \left(\mathbf{C}^{-1}\otimes\mathbf{C}^{-1}\right)^{T_{23}}\right)\\ - \mathbf{C}^{-1}\otimes\mathbf{I} - \mathbf{I}\otimes\mathbf{C}^{-1}\Bigg].\end{aligned} \tag{16}$$

In Eq. (16), the operator $(\cdot)^{T_{ij}}$ stands for special transposition; i.e. exchange of the i-th with the j-th base system.

The evaluation of the remaining part

$$-\rho_0\frac{\partial \psi_{\mathrm{d}}}{\partial q_{\mathrm{d}}}\,\dot{q}_{\mathrm{d}} - \rho_0\frac{\partial \psi_{\mathrm{c}}}{\partial c}\,\dot{c} - \mathbf{j}\cdot\operatorname{Grad}\frac{\partial \psi_{\mathrm{c}}}{\partial c} - \frac{\partial \psi_{\mathrm{c}}}{\partial c}\,\operatorname{Div}\mathbf{j} \geq 0 \tag{17}$$

of the entropy inequality is treated similar to [6,16]. According to the part related to ψ_{d}, one can assume a linear approach

$$\mu(q_{\mathrm{d}}) = \mu_0\,(1 - q_{\mathrm{d}}) \tag{18}$$

for the dependence of the material parameter of the primary network on the internal variable q_{d}, where μ_0 is the shear modulus of unaged elastomer. Regarding the internal variables q_{d} and q_{r}, an evolution equation is needed, which is depending on the absolute temperature θ and on the dimensionless local oxygen concentration c

$$\begin{aligned}\dot{q_{\mathrm{d}}} &= \nu_{\mathrm{d}}\,e^{-\frac{E_{\mathrm{d}}}{R\theta}}\,(1 - q_{\mathrm{d}})\,c, \quad q_{\mathrm{d}}(0) = 0\\ \dot{q_{\mathrm{r}}} &= \nu_{\mathrm{r}}\,e^{-\frac{E_{\mathrm{r}}}{R\theta}}\,(1 - q_{\mathrm{r}})\,c, \quad q_{\mathrm{r}}(0) = 0.\end{aligned} \tag{19}$$

In these equations, R represents the universal gas constant and the parameters ν_{d}, ν_{r} and E_{d}, E_{r} are pre-exponential factors and activation energies. The remaining part of the inequality (17) related to ψ_{c} is combined with the diffusion–reaction equation (1), which leads to

$$-\frac{\partial \psi_{\mathrm{c}}}{\partial c}\,\hat{c} - \mathbf{j}\cdot\operatorname{Grad}\frac{\partial \psi_{\mathrm{c}}}{\partial c} \geq 0. \tag{20}$$

Using a quadratic approach for $\psi_{\mathrm{c}} = \frac{1}{2}\,\alpha\,c^2$ with the non-negative proportionality constant α, this inequality takes the form

$$-\alpha\,c\,\hat{c} - \alpha\,\mathbf{j}\cdot\operatorname{Grad} c \geq 0 \tag{21}$$

and is fulfilled for the constitutive relations

$$\begin{aligned}\hat{c} &= -k(\hat{\Pi})\,c\\ \mathbf{j} &= -d_c(\hat{\Pi})\,\operatorname{Grad} c.\end{aligned} \tag{22}$$

In [16], also higher polynomials are formulated as possible approaches for the chemical part ψ_{c} of the free energy, which lead to mutually bonded thermodynamically consistent constitutive equations for the reaction term, diffusion flux and the heat flux. With respect to the reaction term $\hat{c}$, an ageing-dependent reaction of the oxygen with the elastomer network has been proposed as well

$$k = \left[k_{01}(1 - q_{\mathrm{d}}) + k_{02}(1 - q_{\mathrm{r}})\right]\,e^{-\frac{E_k}{R\theta}}. \tag{23}$$

Table 1 Components of the NBR mixture

Component	Amount (phr)
NBR 1846	100
Filler (carbon black N 550)	60
Plasticizer (DEHP)	20
Antioxidant (6-PPD)	2
Zinc oxide	5
Stearic acid	1
Sulphur	2
CBS	1.5
TMTM-80	0.5

Here, the reaction term becomes a function of the temperature θ and the internal variables q_d, q_r. On the one hand, the reaction rate k increases with higher temperature and, on the other hand, the reactivity is slowed down locally with increasing state of ageing. If the two ageing processes (the network degradation and reformation) are completed ($q_\mathrm{d} = 1$, $q_\mathrm{r} = 1$), no more reaction and thus no further oxygen consumption in the elastomer takes place. In such a case, the diffusion–reaction equation (1) becomes a pure diffusion equation. Further diffusion of oxygen into the elastomer is possible, but no chemical reaction is triggered. In Eq. (23), k_{01} and k_{02} are the base parameters and E_k is the activation energy of ageing resp. of oxygen consumption, which have to be identified.

Regarding the diffusion flux $\mathbf{j}$ [see Eq. $(22)_1$], the diffusion coefficient d_c can also be formulated as ageing dependent. First, however, its ageing dependence is studied experimentally and based on the results, a constitutive approach is formulated.

3 Experimental investigations

This section describes the experimental investigations and presents the results. The associated model parameters were also identified on the basis of the measurement results. Following experimental methods have been carried out:

- long-term continuous relaxation tests
- intermittent monotonic tests
- micro-hardness tests
- permeation tests

Nitrile butadiene rubber was prepared according to the formulation shown in Table 1. Following specimen geometries were prepared for the individual experiments: a rectangular-shaped *laboratory specimen* with dimensions of approximately 5 mm × 2 mm × 50 mm, a prismatic-shaped *component-like specimen* with larger dimensions of approximately 10 mm × 10 mm × 60 mm and a circular *membrane* with diameter of 38.5 mm and thickness about 200 μm.

3.1 Long-term continuous relaxation tests

This type of experiment represents a relaxation test, which runs over a larger time scale (e.g. 1000 h). The sample is deformed up to a constant strain, and the stress response is recorded. A stress drop is observed after a certain time, which may be more or less pronounced depending on the material and testing temperature. However, while in the classical relaxation test, the stress drop is caused by viscoelastic effects; the reason in this long-term experiment is based on chemical degradation of the primary network. Network reformation does not contribute, because the secondary network develops stress-free under constant strain in time. This experiment is commonly carried out at different temperature levels so that the temperature dependence of the degradation process is taken into account. In this work, the laboratory specimens were tested in air and the ageing temperatures are 120 °C, 100 °C and 80 °C.

The thickness of the laboratory specimens used in this experiment was chosen to be quite thin (about 0.8 mm), since in that case, the DLO-effect can be neglected during the thermo-oxidative ageing. This will simplify the procedure of parameter identification of network degradation, so that the oxygen concentration

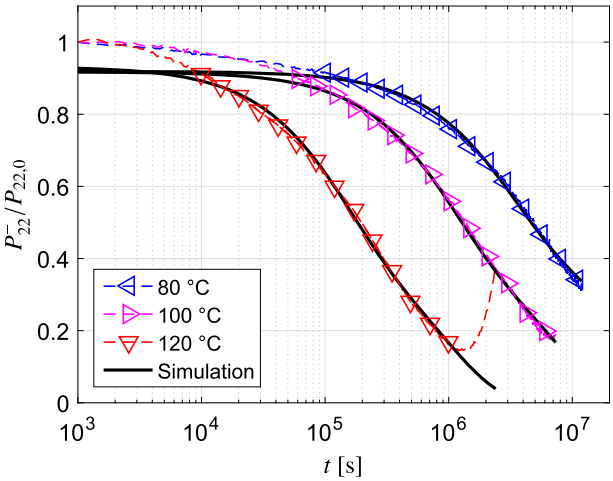

Fig. 1 Continuous relaxation tests and related simulations

in the specimen domain is assumed to be constant and equal to the concentration on the specimen boundary. Thus, a dimensionless concentration c is defined

$$c = \frac{c_0}{\bar{c}}, \quad 0 \leq c \leq 1, \tag{24}$$

where c_0 is the local oxygen concentration and $\bar{c}$ is the concentration on the specimen boundary. In case of homogeneous ageing of thin specimens, the dimensionless concentration equals one, and the evolution Eq. (19) take a simplified form

$$\begin{aligned} \dot{q_\mathrm{d}} &= \nu_\mathrm{d}\, e^{-\frac{E_\mathrm{d}}{R\theta}} (1 - q_\mathrm{d}) \\ \dot{q_\mathrm{r}} &= \nu_\mathrm{r}\, e^{-\frac{E_\mathrm{r}}{R\theta}} (1 - q_\mathrm{r}). \end{aligned} \tag{25}$$

Results of the continuous relaxation tests are plotted in the Fig. 1. One can observe a pronounced temperature-dependent decrease in the measured first Piola-Kirchhoff stress P_{22}^{-} (so-called engineering stress) in time, which is normalized with its value $P_{22,0}$ at the beginning. For parameter identification one can use an approach in which the obtained stress P_{22}^{-}

$$\begin{aligned} P_{22}^{-} &= P_{22,0}\,(1 - q_\mathrm{d}) \\ q_\mathrm{d} &= \frac{1}{n} \sum_{j=1}^{n} q_\mathrm{d}^{j} \end{aligned} \tag{26}$$

depends on the internal variable q_d in the same sense as the shear modulus $\mu(q_\mathrm{d})$ (Eq. 18). Taking the analytical solution of Eq. $(25)_1$ for isothermal conditions into account, the parameters of the network degradation process, i.e. E_d^{j} and ν_d^{j}, are identified. Simulations using the model with the identified parameters are also shown in Fig. 1, whereby a good match is visible. Since the fit has been provided for the range of a long-term behaviour (fitting points are denoted with triangles), the short-time viscoelastic effects have been omitted.

3.2 Intermittent monotonic tests

According to the intermittent experiments, thin laboratory specimens are stored under the same thermal and chemical boundary conditions as in the aforementioned continuous relaxations tests. The only difference is the stress-free ageing. These tests are used to investigate the network reformation process, so that after certain times, ageing is intermittent and the specimens are cooled down to the room temperature. With such a pre-aged specimen, a suitable mechanical experiment can be carried out at room temperature. In this study, slow monotonic uni-axial tensile tests are provided, whereby the strain rate is constant (about 0.001%/s), such that possible influences of ageing on viscoelasticity were not investigated. Some of the tensile curves are presented in Fig. 2. Based on the results of the continuous relaxation tests (Sect. 3.1), one could assume that the material

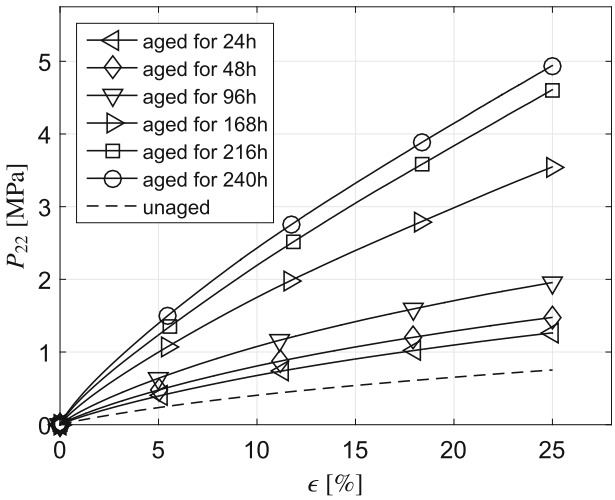

Fig. 2 Stress–strain curves of NBR specimens aged in air at 120 °C

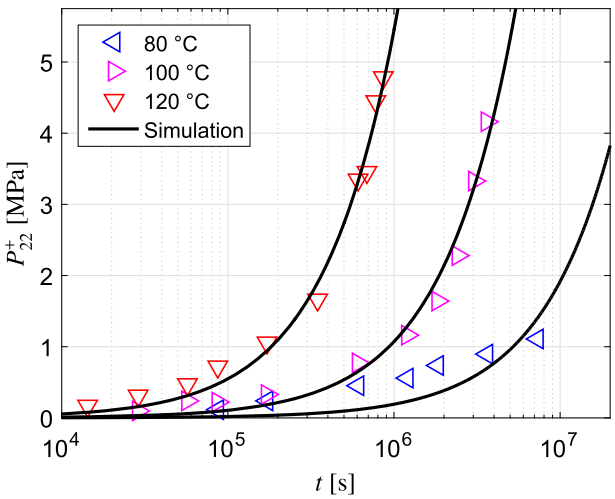

Fig. 3 Stress of the reformed network in NBR specimens aged in air, evaluated at 25% strain, and related simulations

stiffness decreases significantly during ageing. The intermittent tensile tests, however, have shown the contrary, so that one can observe an increase in stiffness with an increasing ageing state. As a result, network reformation presents a dominant process during ageing.

To obtain only the evolution of the reformed network, the measured tensile curves are evaluated at different strains and the contribution of the network degradation is subtracted. The evolution of the stress P_{22}^{+} of the reformed network over the ageing time at those three ageing temperatures is presented in Fig. 3. Thus, the parameters of the network reformation process, i.e. E_{r}^{j} and ν_{r}^{j}, are identified using an approach for the stress P_{22}^{+} as

$$\begin{aligned} P_{22}^{+} &= q_{\mathrm{r}}\, P_{22,\infty}, \\ q_{\mathrm{r}} &= \frac{1}{n}\sum_{j=1}^{n} q_{\mathrm{r}}^{j} \end{aligned} \tag{27}$$

and taking the analytical solution of Eq. $(25)_2$ for isothermal conditions into account. For more details, according to the parameter identification of the network reformation and degradation, see [15]. The shear modulus μ_0 of the unaged NBR was identified directly from the stress–strain curve denoted with a dashed line in Fig. 2.

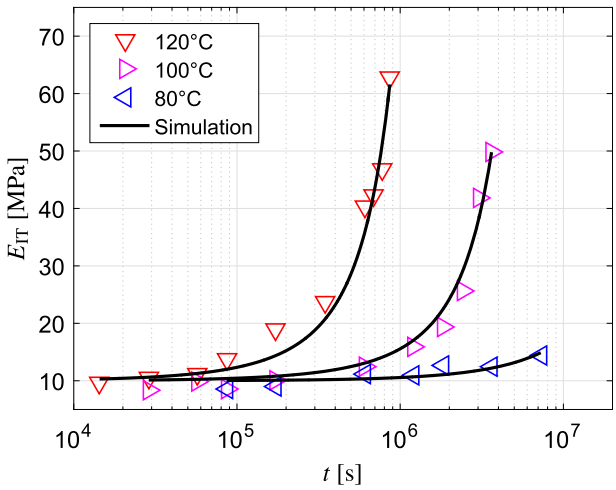

Fig. 4 Results of the micro-hardness tests on aged laboratory specimens and related simulations

3.3 Micro-hardness tests

For further ageing studies, micro-hardness tests were used. According to [11], such tests, as well as uni-axial tensile tests, are suitable for determining the activation energy of oxygen consumption present in Eq. (23). The advantage of the micro-hardness testing is that the recorded data at the sample surface are not affected by DLO-induced inhomogeneities. Before the tensile tests where carried out, the pre-aged thin laboratory specimens from Sect. 3.2 were tested by means of instrumented micro-hardness testing according to the European standard EN ISO 14577. For each specimen, measurements at several positions on the specimen surface were carried out, the controlled testing load being set to 25 mN. A Vickers indenter was used, so that the elastic indentation modulus E_{IT}, which is comparable to the Young's modulus of the material to be examined, can be calculated. As a result (see Fig. 4), one obtains a dependence of the indentation modulus on the ageing duration for different ageing temperatures. Based on the test results, the data are fitted using an exponential function

$$\sigma = \sigma_0 \, e^{-\frac{t}{\tau(\theta)}} . \tag{28}$$

Hence, the temperature-dependent relaxation times $\tau(\theta)$ are identified. In order to describe the temperature dependence of the ageing process, the obtained relaxation times are plotted in an Arrhenius diagram (Fig. 5). It can be clearly seen that the thermal behaviour of ageing, resp. of the chemical reactions taking place, exhibits an Arrhenius behaviour. Hence, using an Arrhenius equation

$$\tau(\theta) = a_0 \, e^{\frac{E_k}{R\,\theta}} , \tag{29}$$

the activation energy E_k of the oxygen consumption can be determined. The identified values correlate with the results for the nitrile rubber obtained by Gillen et al. [11].

3.4 Permeation tests

Permeation measurements are used to study the diffusion properties of gases in elastomers. In general, the permeability P, the solubility S and the diffusion coefficient d_{c} of a particular gas into the elastomer can be determined. At first, an elastomer membrane is mounted in a permeation cell and the membrane is degassed for at least 24 h in high vacuum ($< 10^{-3}$ Pa). Below the membrane, at the so-called downstream side, a known volume is attached in which the pressure can be measured with high accuracy using a capacitance manometer. In order to perform the permeation experiment, the upstream side of the initially gas-free membrane is instantaneously exposed to a well-defined gas pressure p_{upper}. Due to diffusive transport along the concentration gradient across the membrane thickness, the gas permeates into the previously evacuated downstream volume and results in a corresponding pressure increase. The downstream pressure p_{down} is recorded as function of time. The slope of the resulting curve is increasing until a steady state of diffusion is reached, and the slope of this state is

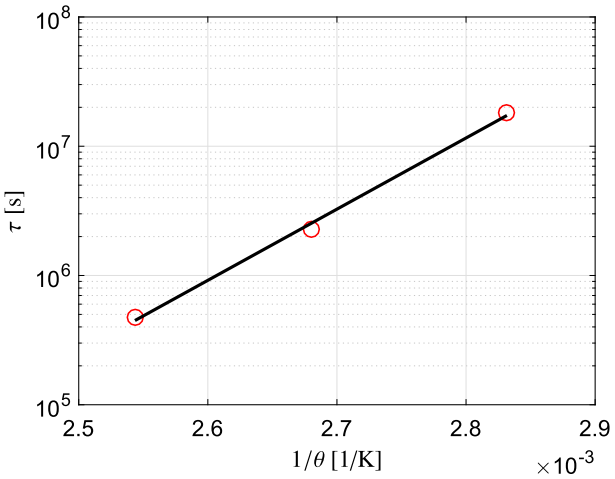

Fig. 5 Arrhenius diagram and determination of the activation energy of oxygen consumption

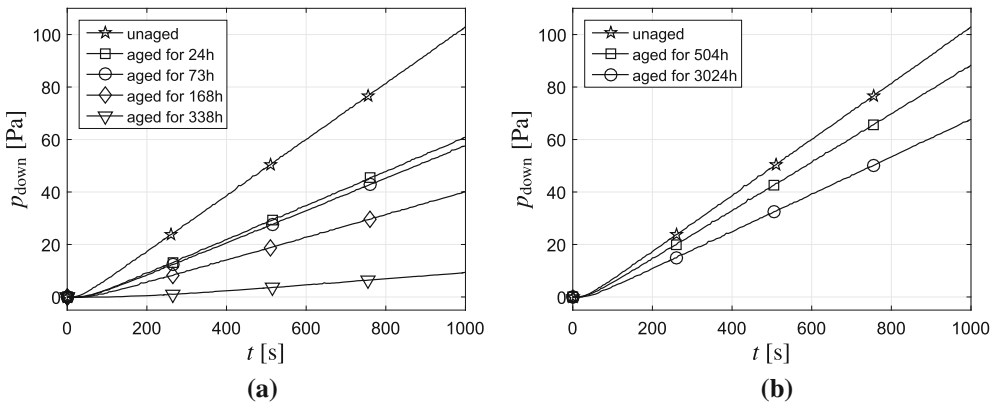

Fig. 6 Permeation tests; pressure increase curves for specimens aged at **a** 120 °C, **b** 80 °C

related to the permeability coefficient. Permeation cell and upstream and downstream volumes are placed in an air bath by which a constant temperature of 35 °C is maintained.

In order to study the development of the DLO-effect, permeation tests were run on unaged and aged NBR membranes. Resulting curves are shown in Fig. 6 for the oxygen permeability at 0.1 MPa oxygen pressure. It can be clearly seen that the slope of the curves decreases with more pronounced state of ageing, which is linked to the decreasing permeability. Similar permeation behaviour on the aged elastomers has been observed by Kömmling et al. [18] and Steinke [28]. The reason for this is the influence of increasing cross-linking density and the associated change in the permeation and diffusion behaviour.

To determine the diffusion coefficient from the measured pressure increase curve, the time-lag method (cf. [5,25]) is usually used. The first transient part of the curve is related to the time needed to establish a constant concentration profile across the membrane thickness giving rise to the steady state permeability. If the membrane was initially gas-free, this time-lag, i.e. the intercept of the steady state slope with the time-axis, allows for the determination of an effective diffusion coefficient. However, it is also possible to identify the diffusion coefficient by using a numerical solution of the diffusion equation coupled with a nonlinear optimization algorithm. Within the optimization procedure, the diffusion equation is solved across the membrane thickness L. As boundary conditions, the two pressures from the permeation test are used. The Henry's law is applied to describe the oxygen concentration on the upstream side of the membrane $c(0,t) = p_{\text{upper}}\, S$ and on the downstream side $c(L,t) = p_{\text{down}}\, S$. The ideal gas equation applies for the pressure in the downstream volume

$$p_{\text{down}} = \frac{R\,\theta}{V_{\text{down}}}\, q, \tag{30}$$

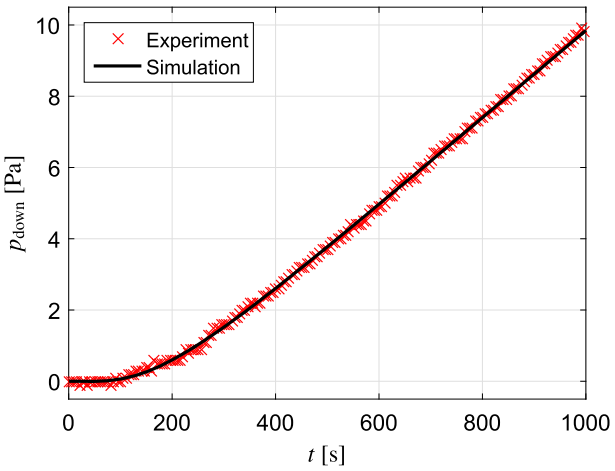

Fig. 7 Identification of the diffusion coefficient and the solubility from the pressure increase curve

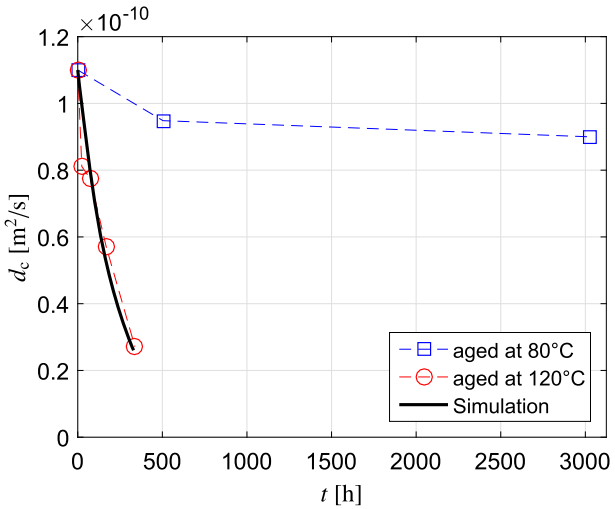

Fig. 8 Diffusion coefficients for different ageing times and temperatures, with related simulation

where θ is the testing temperature and V_{down} is the volume of the downstream side. According to [31], the quantity

$$q = A \int_0^t j \, \mathrm{d}t = -A \, d_c \int_0^t \frac{\partial c}{\partial x} \, \mathrm{d}t \tag{31}$$

is the amount of diffusing substance passing a section of surface area A of the membrane in total time t. Equations (30) and (31) lead to the expression

$$p_{\mathrm{down}} = -\frac{R \, \theta \, A}{V_{\mathrm{down}}} \, d_c \int_0^t \frac{\partial c}{\partial x} \, \mathrm{d}t, \tag{32}$$

in which $\partial c / \partial x$ is the concentration gradient of oxygen on the downstream membrane side and is calculated for each time step of the solution. The two unknown parameters S and d_c are optimized such that the error between the calculated p_{down} from Eq. (32) and the measured pressure increase is minimized (see Fig. 7). The results achieved by the numerical method were congruent with the results of the time-lag method.

The dependence of the diffusion coefficients on the ageing time and ageing temperature is presented in Fig. 8. At the ageing temperature of 120 °C, the diffusion coefficient decreases significantly with the ageing time, indicating an increased reaction of the elastomer network with oxygen. At the lower ageing temperature of 80 °C, the diffusion coefficient behaves almost constant over the ageing time of about 500 h, such that the

influence of an increasing cross-linking density can be neglected here. Thus, diffusion behaviour at 120 °C can be empirically described as ageing dependent

$$d_{\mathrm{c}} = d_{\mathrm{c},0}\, e^{-\gamma_{\mathrm{c}}\, q_{\mathrm{r}}}. \tag{33}$$

It is a nonlinear function of the ageing variable q_{r} which describes the network reformation process. In this equation, $d_{\mathrm{c},0}$ represents the diffusion coefficient of unaged NBR; the parameter γ_{c} has to be identified. An affiliated simulation is plotted in Fig. 8.

Generally, the diffusion coefficient plays an important role in case of thermo-oxidative ageing, in which it exhibits a pronounced ageing dependence especially at high temperature levels. This leads to a reduction in the oxygen diffusivity at the more oxidized elastomer surface regions. Despite the local deceleration of the diffusion, this knowledge alone is not sufficient enough to describe the DLO-effect. Even with a decrease in the diffusion coefficient by approximately 80%, as it has been observed for the case of ageing at 120 °C, an elastomer component would be finally completely saturated with oxygen. The time to reach such a steady state would, of course, take longer than in the case of a moderate ambient temperature, at which the reaction rate of the oxygen molecules with the elastomer is low. In order to represent the DLO-effect, it is therefore very important to identify also the reaction properties.

4 Parameter identification and numerical simulations

This section deals with the numerical conversion of the proposed constitutive model and identification of its reaction term. The influence of antioxidant on thermo-oxidative ageing will also be examined and a validation example with the implemented and identified material model is included.

4.1 Numerical implementation

The equations to be solved are implemented as a multifield problem in the commercial FE-software Comsol Multiphysics. The balance of momentum, the diffusion–reaction equation and the evolution Eqs. (13), (19) have to be transferred into the weak form. Therefore, the equations are multiplied by test functions and integrated over the volume Ω of the body, which leads after several mathematical steps to the following equations

$$\begin{aligned}
&\int_{\Omega} \mathbf{S} : \delta\mathbf{E}\, \mathrm{d}\Omega = \int_{\Gamma} \mathbf{t} \cdot \delta\mathbf{u}\, \mathrm{d}\Gamma \\
&\int_{\Omega} \left(\rho_0\, \dot{c} - \hat{c}\right)\, \delta c\, \mathrm{d}\Omega - \int_{\Omega} \mathbf{j} \cdot \mathrm{Grad}(\delta c)\, \mathrm{d}\Omega = -\int_{\Gamma} \tilde{j}\, \mathrm{d}\Gamma \\
&\int_{\Omega} \left(\dot{\mathbf{S}}_{\mathrm{r}} - \frac{1}{2}\, q_{\mathrm{r}}(t)\, \overset{4}{\mathbf{D}}\,(t) : \dot{\mathbf{C}}\right) : \delta\mathbf{S}_{\mathrm{r}}\, \mathrm{d}\Omega = 0 \\
&\int_{\Omega} \left(\dot{q}_{\mathrm{d}} - \nu_{\mathrm{d}}\, e^{-\frac{E_{\mathrm{d}}}{R\theta}} (1 - q_{\mathrm{d}})\, c\right)\, \delta q_{\mathrm{d}}\, \mathrm{d}\Omega = 0 \\
&\int_{\Omega} \left(\dot{q}_{\mathrm{r}} - \nu_{\mathrm{r}}\, e^{-\frac{E_{\mathrm{r}}}{R\theta}} (1 - q_{\mathrm{r}})\, c\right)\, \delta q_{\mathrm{r}}\, \mathrm{d}\Omega = 0,
\end{aligned} \tag{34}$$

which are based on the total Lagrangian formulation. The primary variables such as the displacement field $\mathbf{u}$ and the dimensionless concentration field c are discretized using Lagrangian shape functions with quadratic element order for $\mathbf{u}$ and linear element order for c. According to the stress tensor $\mathbf{S}_{\mathrm{r}}$ and the internal variables q_{d}, q_{r}, discontinuous Lagrange discretization is used to speed up the computation, the shape function order is one order less than what is used for the displacements. This results in a smaller number of extra degrees of freedom which are added to the model in comparison with Gauss point data, whereby the accuracy does not differ in general. The Neumann boundary conditions $\mathbf{t}$ and $\tilde{j}$ can be prescribed on the body's surface Γ. Since the related multifield problem is time-dependent, the corresponding discretized ordinary differential equations are solved with the implicit time-integration backward differential method of the second order.

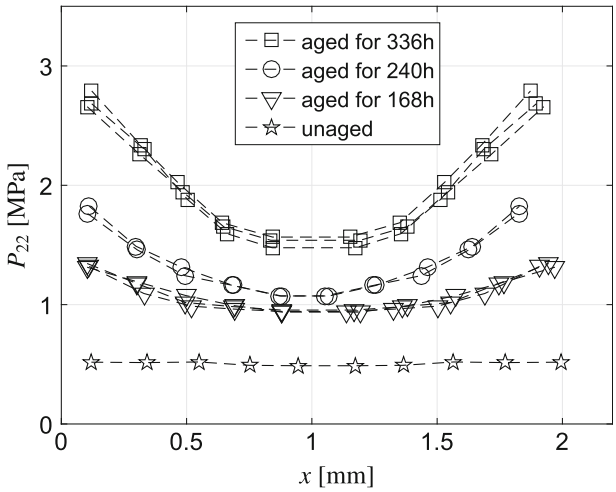

Fig. 9 Stress profiles across the NBR-specimens thickness aged at 120 °C

4.2 Identification of reaction term

Since all required parameters of the constitutive model and as well the ageing-dependent diffusion coefficient have already been identified with the help of individual experimental methods, the identification of the base parameters k_{01} and k_{02} of the reaction term [see Eq. (23)] remains. For this purpose, an indirect identification procedure in the sense of inverse FEM will be applied.

At first, a set of NBR plates with much larger lateral dimensions than their thickness (approx. 2 mm) is aged under zero stress in air at 120 °C for different durations. This ensures that a one-dimensional diffusion or ageing state occurs in the middle part of the plate. Rectangular-shaped specimens are then stamped out of the middle of the aged plates. Using a splitting machine designed by the Fortuna company, the stamped specimens are split into individual thin layers, with a thickness of approximately 200 μm. With such layers, one can perform a suitable mechanical experiment, whereby in this study, monotonic uni-axial tensile tests using a strain rate of 0.001%/s has been provided.

The obtained tensile curves are evaluated at certain strains along the initial specimen thickness of about 2 mm, which results in an inhomogeneous stress profile across the elastomer specimen plotted in Fig. 9. For a better comparison, a profile of the engineering stress is also created for an unaged specimen such that a constant stress distribution can be observed. In case of aged specimens, the stress reaches maximum values in the outer layers and then decays in the direction to the middle of the specimen. This inhomogeneous stress distribution is a clear indicator of the DLO-effect. An increasing oxygen reaction takes place at the periphery of the elastomer and only a reduced oxidation in its interior, since the atmospheric oxygen is consumed faster at the edges and only the non-reacted oxygen is available to be further supplied by diffusion transport. This effect is of course dimension-dependent and would by more pronounced in components of larger dimensions. The ageing-dependent diffusion coefficient also plays a role, because diffusion is slowed down locally. In order to provide some statistical information, stress profiles were created in all three ageing situations (168 h, 240 h and 336 h) for several specimens, whereby a good reproducibility of the DLO-effect is visible.

In order to identify the base parameters of the reaction term, a boundary value problem (BVP) is computed using the implemented material model. It is a tensile test with an inhomogeneously aged NBR specimen as shown in Fig. 10. A 2D model of the specimen geometry with the corresponding thickness of approx. 2 mm is built up. The thickness area of the specimen is modelled and calculated in plane-stress mode. In the first simulation step, inhomogeneous load-free ageing in air at 120 °C is simulated, such that the dimensionless oxygen concentration ($c = 1$) is prescribed only at the side boundaries of the specimen. At the upper and lower boundary, the concentration flux equals zero and the oxygen can therefore only diffuse in one direction, which corresponds to a one-dimensional diffusion–reaction state. In the second simulation step, after the ageing phase, a uni-axial tensile test is simulated, in which the displacement u_2 is prescribed on the upper boundary. The resulting stress distribution is plotted in Fig. 10. This FE simulation is executed within the optimization procedure using genetic algorithm, and the parameters k_{01} and k_{02} are optimized in such a way that the error between the measured and calculated stress distribution is minimized. This indirect identification method has

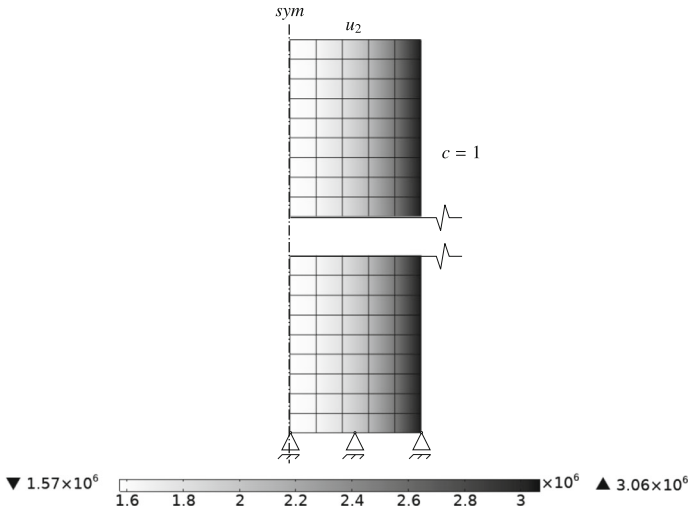

Fig. 10 BVP with applied boundary conditions; computed stress distribution P_{22} in MPa

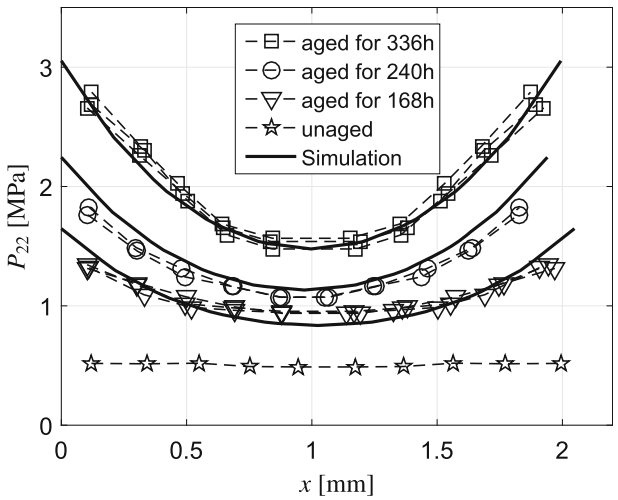

Fig. 11 FE simulations of the stress profiles across the NBR-specimens thickness aged at 120 °C

led to very good results presented in Fig. 11. The simulation curves run above the measured data in the sense of extrapolating them to the specimen edges. Each measurement point represents an average value of the measured stress of the individual thin layer and is plotted as a marker in the middle of the layer thickness. The thinner a layer can be produced, the better the resolution towards the specimen edge. The selected layer thickness of about 200 μm was the optimum in this case.

4.3 Influence of antioxidants

In spite of the successful fit of the proposed material model to the measured stress profiles caused by the DLO-effect, a slight deviation, especially at the boundary areas of the heterogeneously aged specimen, can be observed for the two lower ageing times (240 h and 168 h). The parameters occurring in the evolution equations of ageing (Eq. 19) were identified using thin laboratory specimens in which a homogeneous ageing state was assumed. A homogeneous ageing state ($c = 1$) therefore corresponds to an ageing state at the surface of an inhomogeneously aged specimen, where $c = 1$ also applies. However, it seems that the ageing rate at the edge of a thicker or inhomogeneously aged specimen is slower. This statement was experimentally verified by ageing a set of specimens consisting of a laboratory specimen and a component-like specimen of larger dimensions in air at 120 °C for various durations. In parallel, the same set of specimens has been

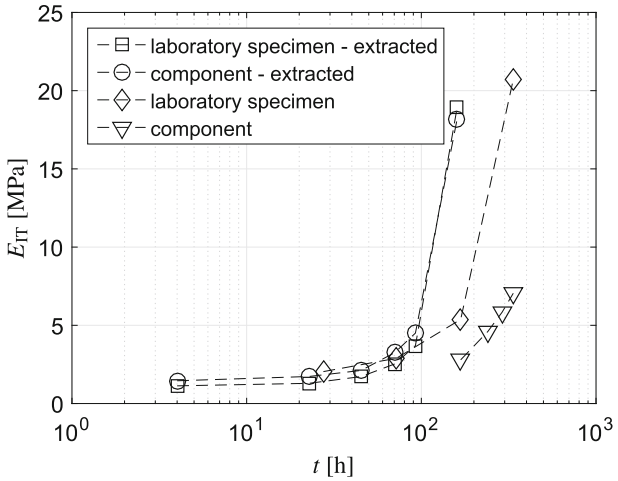

Fig. 12 Surface modulus for various specimens aged at 120 °C

aged under the same ageing conditions, but for the initially unaged elastomers, the antioxidants have been extracted by chemical extraction. At certain times, ageing was interrupted, and the specimens were cooled down to room temperature and then subjected to micro-hardness testing. The micro-hardness or the elastic indentation modulus E_{IT} was measured as an indicator for the ageing state on the elastomer surface and plotted over the ageing time in Fig. 12. For the component and the laboratory specimen, which contain antioxidants, a significant difference in the surface ageing can be observed. On the other hand, the geometry showed no influence in case of extracted specimens and the much larger component shows an almost identical ageing state with respect to the 2-mm-thick laboratory specimen. The influence of antioxidants is therefore not negligible in the chemical ageing of stabilized elastomers. During a heterogeneous oxidation and DLO-effect formation, a gradient of antioxidants can be also created, as it is consumed faster at the edges. In the case of larger-volume components, there is of course a higher amount of the antioxidants present and thus can be supplied from the interior to the edges by a diffusion process. This effect can decelerate the oxidation and the ageing at the surfaces of bigger elastomer components. Thus, this is the reason for the deviation of the simulation, since the surface ageing does not develop in the same way with different specimen geometries. In order to correct these effects, the influence of the antioxidants has to be taken into account in the proposed model.

In this paper, a simple approach is proposed which allows to model the impact of the antioxidants on ageing and ultimately on the material properties. It will be basically considered that two diffusion–reaction processes occur during inhomogeneous ageing; on the one hand, a reaction of oxygen with the elastomer, and on the other hand, the oxygen reacts with the antioxidants, which can be modelled using the two following diffusion–reaction equations (cf. [23])

$$\begin{aligned} \rho_0\,\dot{c} + \mathrm{Div}\,\mathbf{j} - \hat{c} - \hat{c}_{\mathrm{a}} &= 0 \\ \dot{c}_{\mathrm{a}} + \mathrm{Div}\,\mathbf{j}_{\mathrm{a}} - \hat{c}_{\mathrm{a}} &= 0. \end{aligned} \tag{35}$$

The index *a* stands for antioxidants. The entropy flux

$$\boldsymbol{\Phi}^{s} = -\frac{1}{\theta}\left(\frac{\partial \psi}{\partial c}\,\mathbf{j} + \frac{\partial \psi}{\partial c_{\mathrm{a}}}\,\mathbf{j}_{\mathrm{a}}\right) \tag{36}$$

is therefore also affected by the change of antioxidants, and the Clausius–Duhem inequality results in

$$-\rho_0\,\dot{\psi} + \mathbf{S} : \dot{\mathbf{E}} - \mathbf{j}\cdot\mathrm{Grad}\,\frac{\partial \psi}{\partial c} - \frac{\partial \psi}{\partial c}\,\mathrm{Div}\,\mathbf{j} - \mathbf{j}_{\mathrm{a}}\cdot\mathrm{Grad}\,\frac{\partial \psi}{\partial c_{\mathrm{a}}} - \frac{\partial \psi}{\partial c_{\mathrm{a}}}\,\mathrm{Div}\,\mathbf{j}_{\mathrm{a}} \geq 0. \tag{37}$$

The set of process variables is now extended by the dimensionless antioxidant concentration c_{a} ($0 \leq c_{\mathrm{a}} \leq 1$), such that for the diffusion flux $\mathbf{j}_{\mathrm{a}}$ and the reaction term $\hat{c}_{\mathrm{a}}$, constitutive laws have to be formulated as well. Using the approach

$$\psi_{\mathrm{c}} = \frac{1}{2}\,\alpha\left(c^2 + c_{\mathrm{a}}^2\right) \tag{38}$$

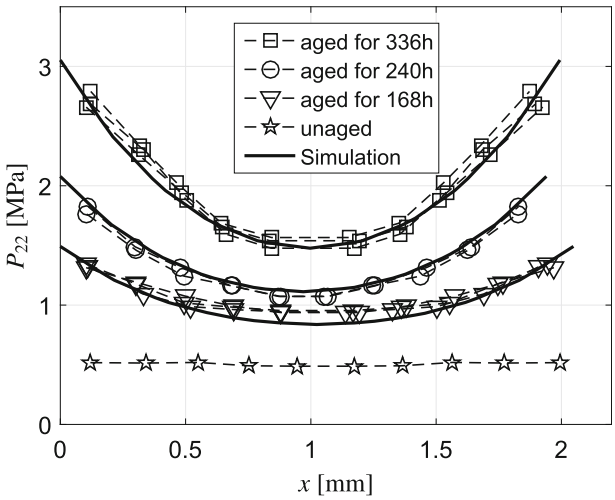

Fig. 13 FE simulations of the stress profiles across the NBR-specimens thickness aged at 120 °C, using the modified material model

for the chemical part ψ_c of the free energy function, the evaluation of the resulting dissipation inequality finally leads to the constitutive relationships:

$$\begin{aligned} \hat{c} &= -k\, c \\ \hat{c}_a &= -k_a\, c\, c_a \\ \mathbf{j} &= -d_c\ \mathrm{Grad}\, c \\ \mathbf{j}_a &= -d_a\ \mathrm{Grad}\, c_a. \end{aligned} \tag{39}$$

Equation (39_2) represents the second-order reaction of oxygen with antioxidants (cf. [1]), where the reaction rate k_a has to be identified. The diffusion coefficient d_a of antioxidants in elastomer was chosen according to [24]. In this way, the oxygen and antioxidant concentration can be calculated in each position and time for an elastomer component during thermo-oxidative ageing.

In order to model the effects of antioxidants on ageing, the evolution Eq. (19) is reformulated

$$\begin{aligned} \dot{q_d} &= \nu_d\, e^{-\frac{E_d}{R\theta}} (1 - q_d)\, c\, (1 - c_a), \quad q_d(0) = 0 \\ \dot{q_r} &= \nu_r\, e^{-\frac{E_r}{R\theta}} (1 - q_r)\, c\, (1 - c_a), \quad q_r(0) = 0, \end{aligned} \tag{40}$$

such that the antioxidant concentration in the elastomer is taken into account. For an initial state or as long as a concentration of $c_a = 1$ is present in the elastomer, the oxidation is inhibited by means of antioxidant and thus, no ageing can occur. In case that there is no antioxidant present, i.e. $c_a = 0$, it can no more contribute to thermo-oxidative ageing and the evolution equations take the form of Eq. (19). With the proposed material model which is extended by the diffusion–reaction equation for the antioxidant and the modified evolution equations, the reaction rates k_{01}, k_{02} and k_a can be identified by using inverse FEM for computing the same BVP (see Fig. 10). As it can be seen in Fig. 13, the proposed treatments have significantly improved the results for the two critical ageing times of 240 h and 168 h.

4.4 Validation and discussion

The identified and implemented material model has been validated including the consideration of antioxidants using the example of an elastomer component. The component-like specimen provides a suitable validation geometry. Due to the 1:1 aspect ratio of its cross-section, the diffusion and reaction processes take place in two dimensions during thermo-oxidative ageing. For the validation experiment, the component was aged under zero stress in air at 120 °C for 240 h and then a three-point bending test was carried out at the room temperature, as shown in Fig. 14. In the same sense, a FE simulation was carried out. The steel stamp and the steel supports of the testing device were modelled as rigid bodies, so that contact boundary conditions could be included in the calculation. The steel stamp was moved in a displacement controlled manner until the desired

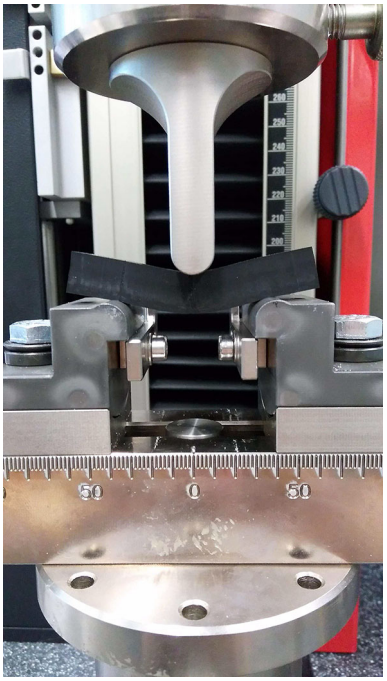

Fig. 14 Three-point bending test with the aged component

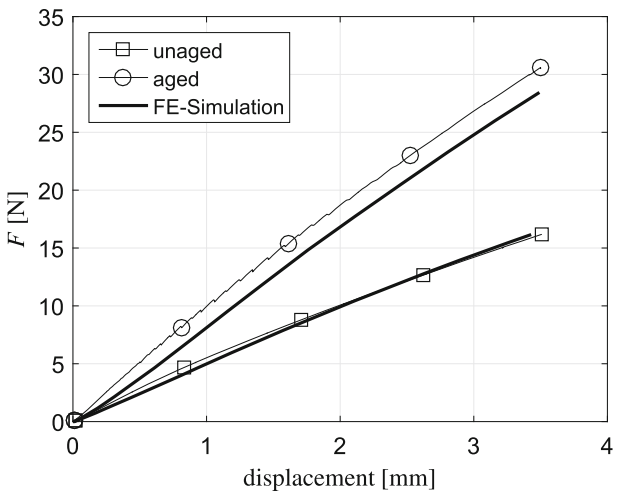

Fig. 15 Results of the three-point bending test with the aged and unaged component

deflection of the component was reached. The force-displacement diagram was recorded and compared with the FE simulation. The validation results, presented in Fig. 15, demonstrate the plausibility of the proposed continuum-mechanical modelling approach and performed experiments. Regarding the aged component, the model slightly underestimates the reality, whereas qualitatively, the results look good with a slight deviation smaller then 10%.

In order to improve the simulation results, the identification of the activation energy of oxygen consumption E_k should be optimized. In this paper, E_k was identified using the surface modulus obtained from laboratory specimens without consideration of the influence of geometry and antioxidants. In the given validation example, a component with a much larger volume has been aged and has thus reached a different state of ageing at the surface. This can also mean a different activation energy. With regard to stabilized elastomers, another identification method for E_k might be advantageous. The deviation of the simulation is also influenced by the choice of the diffusion coefficient of the antioxidants according to the work of [24]. It was not determined

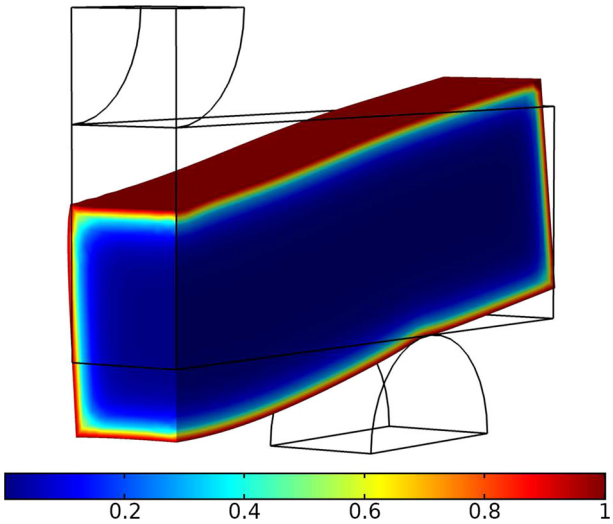

Fig. 16 Quarter model of the bending-loaded component; calculated dimensionless oxygen concentration c

Table 2 Identified model parameters

Parameter	Value	Parameter	Value
μ_0	1.844 MPa	K	$\mu_0 \times 10^3$ MPa
μ_r	567.3 MPa		
E_d^1	8.9732×10^4 J/mol	E_d^2	1.0361×10^5 J/mol
ν_d^1	5.3955×10^6 1/s	ν_d^2	5.401×10^7 1/s
E_r^1	9.5852×10^4 J/mol	ν_r^1	8.745×10^4 1/s
$d_{c,0}$	1.1×10^{-10} m^2/s	k_{01}	2.776×10^7 1/s
γ_c	72.196	k_{02}	2.136×10^{10} 1/s
		E_k	1.0513×10^5 J/mol
$d_{a,0}$	1.082×10^{-8} m^2/s	k_a	2.702×10^{-5} 1/s
E_a	1.694×10^4 J/mol (cf. [24])		

exactly for the NBR and 6-PPD antioxidants used in the mixture. In order to make the identification of the reaction k_a between oxygen and antioxidants more plausible from the chemical point of view, the antioxidant concentration profiles of aged specimens should be measured using the GC-MS method in order to take them into account for the parameter identification. Finally, one should not forget the influence of thermal ageing on the mechanical behaviour of elastomers. Especially in the case of large-volume components, only low oxidation occurs in the inner area and the relevant ageing mechanism can be purely thermal. The same effect can be observed with the aged component (see Fig. 16), where the calculated oxygen concentration after 240 h shows only low values in the interior and the contribution of a pure thermal degradation can gains on importance. This will certainly also influence the slight deviation between the results of the simulation and the validation experiment. Otherwise, the validation of the elastomer component is to be regarded as successful; however, a validation at a lower ageing temperature than 120 °C is still open.

Hence, the modelling and parameter identification strategy of inhomogeneous thermo-oxidative ageing of elastomers still offers some room for improvement.

5 Conclusion

In this paper, the inhomogeneous thermo-oxidative ageing of NBR was experimentally investigated and simulated. A thermodynamically consistent model within the framework of finite hyperelasticity has been formulated taking the diffusion–reaction behaviour of oxygen and the influence of the antioxidants into account. A concept of internal variables has been used to model the impact of ageing on the material properties. All

model parameters have been identified using various experimental methods on aged and unaged NBR specimens and can be found in Table 2. The material parameters, which are related to the ageing model and the diffusion–reaction equations, have been successfully adjusted. The results of the individual simulations match the underlying measurements very well. Subsequently, the resulting partial differential equations, evolution equations and constitutive equations of the multifield problem to be solved were implemented in a commercial FE software. Based on the simulation of the inhomogeneous ageing and bending loading of an elastomer component, the continuum-mechanical modelling approach has been successfully validated.

Hence, the capability of the model to simulate this complex material behaviour was shown and some possible improvements have been discussed. In the case of industrial applications, this model can be used to simulate the inhomogeneous chemo-mechanical ageing of elastomers taking DLO-effect into account and thus to depict the impact on material properties in time, which may be necessary for a lifetime prediction of the rubber components.

Acknowledgements The financial support of the project by the Deutsche Forschungsgemeinschaft (DFG) under the Grant Number JO 818/3-1 is gratefully acknowledged.

References

1. Atkins, P., De Paula, J.: Physical Chemistry: Thermodynamics, Structure, and Change, 8th edn. Oxford University Press, Oxford (2006)
2. Audouin, L., Langlois, V., Verdu, J., de Bruijn, J.: Review: role of oxygen diffusion in polymer ageing: kinetic and mechanical aspects. J. Mater. Sci. **29**, 569–583 (1994)
3. Blum, G., Shelton, J., Winn, H.: Rubber oxidation and ageing studies. Ind. Eng. Chem. **43**, 464–471 (1951)
4. Bolland, J.: Kinetics of olefin oxidation. Q. Rev. Chem. Soc. **3**, 1–21 (1949)
5. Crank, J., et al.: The Mathematics of Diffusion. Oxford University Press, Oxford (1979)
6. Dippel, B., Johlitz, M., Lion, A.: Ageing of polymer bonds: a coupled chemomechanical modelling approach. Contin. Mech. Thermodyn. **26**, 247–257 (2014)
7. Duarte, J., Achenbach, M.: On the modelling of rubber ageing and performance changes in rubbery components. Kaut. Gummi Kunstst. **60**, 172–175 (2007)
8. Ehrenstein, G., Pongratz, S.: Beständigkeit von Kunststoffen. Carl Hanser Verlag, Munich (2007)
9. Flory, P.J.: Thermodynamic relations for high elastic materials. Trans. Faraday Soc. **57**, 829–838 (1961)
10. Gillen, K.T., Clough, R.L.: Rigorous experimental confirmation of a theoretical model for diffusion-limited oxidation. Polymer **33**, 4358–4365 (1992)
11. Gillen, K.T., Clough, R.L., Wise, J.: Prediction of Elastomer Lifetimes from Accelerated Thermal-Aging Experiments. ACS Publications, Washington (1996)
12. Herzig, A., Johlitz, M., Lion, A.: An experimental set-up to analyse the oxygen consumption of elastomers during ageing by using a differential oxygen analyser. Contin. Mech. Thermodyn. (2014). https://doi.org/10.1007/s00161-014-0396-z
13. Hossain, M., Possart, G., Steinmann, P.: A finite strain framework for the simulation of polymer curing. Part I: elasticity. Comput. Mech. **44**, 621–630 (2009)
14. Johlitz, M.: On the representation of ageing phenomena. J. Adhes. **88**, 620–648 (2012)
15. Johlitz, M., Diercks, N., Lion, A.: Thermo-oxidative aging of elastomers: a modelling approach based on a finite strain theory. Int. J. Plast. **63**, 138–151 (2014)
16. Johlitz, M., Lion, A.: Chemo-thermomechanical ageing of elastomers based on multiphase continuum mechanics. Contin. Mech. Thermodyn. **25**, 605–624 (2013)
17. Johlitz, M., Retka, J., Lion, A.: Chemical ageing of elastomers: experiments and modelling. Const. Models Rubber **7**, 113–118 (2011)
18. Kömmling, A., Jaunich, M., Wolff, D.: Effects of heterogeneous aging in compressed HNBR and EPDM O-ring seals. Polym. Degrad. Stab. **126**, 39–46 (2016)
19. Lee, E.H.: Elastic-plastic deformation at finite strain. J. Appl. Mech. **36**, 1–6 (1969)
20. Lion, A., Johlitz, M.: On the representation of chemical ageing of rubber in continuum mechanics. Int. J. Solids Struct. **49**, 1227–1240 (2012)
21. Nasdala, L., Kaliske, M., Rothert, H.: Entwicklung vonMaterialmodellen zur Alterung von Elastomerwerkstoffen unterbesonderer Berücksichtigung des Sauerstoffeinflusses. Mitteilungen des Instituts für Statik und Dynamik der Universität Hannover, Universität Hannover (2005)
22. Naumann, C.: Chemisch-mechanisch gekoppelte Modellierung und Simulation oxidativer Alterungsvorgänge in Gummibauteilen. Dissertation, TU Chemnitz (2016)
23. Naumann, C., Ihlemann, J.: Chemomechanically coupled finite element simulations of oxidative ageing in elastomeric components. Const. Models Rubber **8**, 43–49 (2013)
24. Pushpa, S., Goonetilleke, P., Billingham, N.: Diffusion of antioxidants in rubber. Rubber Chem. Technol. **68**, 705–716 (1995)
25. Rutherford, S., Do, D.: Review of time lag permeation technique as a method for characterisation of porous media and membranes. Adsorption **3**, 283–312 (1997)
26. Shaw, J., Jones, S., Wineman, A.: Chemorheological response of elastomers at elevated temperatures: experiments and simulations. J. Mech. Phys. Solids **53**, 2758–2793 (2005)

27. Simo, J.C., Taylor, R.L.: Penalty function formulations for incompressible nonlinear elastostatics. Comput. Methods Appl. Mech. Eng. **35**, 107–118 (1982)
28. Steinke, L.: Ein Beitrag zur Simulation der thermo-oxidativen Alterung von Elastomeren. VDI-Verlag, Hannover (2013)
29. Steinke, L., Veltin, U., Flamm, M., Lion, A., Celina, M.: Numerical analysis of the heterogeneous ageing of rubber products. In: Jerrams, S., Murphy, N. (eds.) Constitutive Models for Rubber VII, pp. 155–160. CRC Press, Boca Raton (2011)
30. Tobolsky, A.V.: Mechanische Eigenschaften und Struktur von Polymeren. Berliner Union, Stuttgart (1967)
31. Van Amerongen, G.: Diffusion in elastomers. Rubber Chem. Technol. **37**, 1065–1152 (1964)
32. Wise, J., Gillen, K., Clough, R.: Quantitative model for the time development of diffusion-limited oxidation profiles. Polymer **38**, 1929–1944 (1997)